Reprinted from the Preprint Volume of the Ninth Conference on Numerical Weather Prediction, October 14-18, 1991, Denver, Colo. Published by the American Meteorological Society, Boston, Mass.

P1.10

ON THE NORMAL MODES OF LAPLACE'S TIDAL EQUATIONS FOR ZONAL WAVENUMBER ZERO

H. L. Tanaka

Geophysical Institute
University of Alaska Fairbanks
Fairbanks, Alaska

and Akira Kasahara

National Center for Atmospheric Research
Boulder, Colorado

1. Introduction

In recent years, the normal modes of Laplace's tidal equations, referred to as the Hough harmonics, have been applied to the problem of data initialization (Errico 1989), to the numerical integrations of the global shallow-water equations (Kasahara 1977; Salby *et al.* 1990), and to the diagnosis of global atmospheric energetics (Kasahara and Puri 1981; Tanaka 1985; Tanaka and Sun 1990).

For nonzonal motions Hough harmonics are discrete and orthogonal. However, the case of zonal wavenumber zero is special in that the frequencies of gravity modes (first kind) appear as pairs of positive and negative values of the same magnitudes, and the frequencies of the rotational modes (second kind) are all zero. Therefore, the rotational modes corresponding to zonal wavenumber m=0 are not unique. It is necessary to have a complete set of the eigenfunctions of zonal rotational motions (i.e., geostrophic modes) in order to expand atmospheric data in terms of a series of Hough harmonics.

Kasahara (1978) constructed a set of geostrophic modes by a series of Legendre polynomials, and applied the Gram-Schmidt procedure to obtain an orthonormal set. These will be referred to as the K-modes. Shigehisa (1983) obtained another type of the geostrophic modes as the limit of rotational modes for $m \to 0$. The limit of the rotational modes is calculated by considering m to be a continuous parameter and the ratio between m and the corresponding eigenfrequency σ to be finite. The latter condition ensures the phase speed $c = \sigma/m$ to be continuous with respect to m. By this approach, Shigehisa obtained orthogonal geostrophic eigensolutions, which are referred to as the S-modes. They have similar characteristics with the rotational modes for $m > 0$. In a software package developed by Swarztrauber and Kasahara (1985), the S-modes are calculated instead of the K-modes.

Since two sets of the geostrophic modes have been proposed, it is meaningful to examine the difference in the properties of the K- and S-modes. We are particularly interested in the spectral characteristics of the observed zonal mean atmospheric states in terms of the two different sets of the geostrophic modes. The atmospheric zonal states are projected onto the two sets of geostrophic modes to complement the normal-mode energetic studies of Tanaka (1985), Tanaka and Kung (1988), and Tanaka and Sun (1990). We used the reanalyzed Level IIIb datasets from the First GARP (Global Atmospheric Research Program) Global Experiment (FGGE) for the Special Observing Period I (SOP-I) provided by the Geophysical Fluid Dynamics Laboratory (GFDL). The differences in the meridional energy spectra are examined to assess the merits of the two sets of geostrophic modes.

2. Normal modes for zonal wavenumber zero

A system of linearized shallow water equations in spherical coordinates of longitude λ and latitude θ for a resting basic state may be reduced to the following eigenvalue problem:

$$L H_m = i\sigma H_m, \tag{1}$$

where L is a matrix differential operator of Laplace's tidal equation and σ is the dimensionless eigenfrequency. The eigensolutions $H_m(\lambda, \theta)$ are referred to as Hough harmonics of wavenumber m and are defined by a product of Hough vector functions $(U, -iV, Z)^T$ and $e^{im\lambda}$. The components U, V, and Z represent the dimensionless longitudinal and

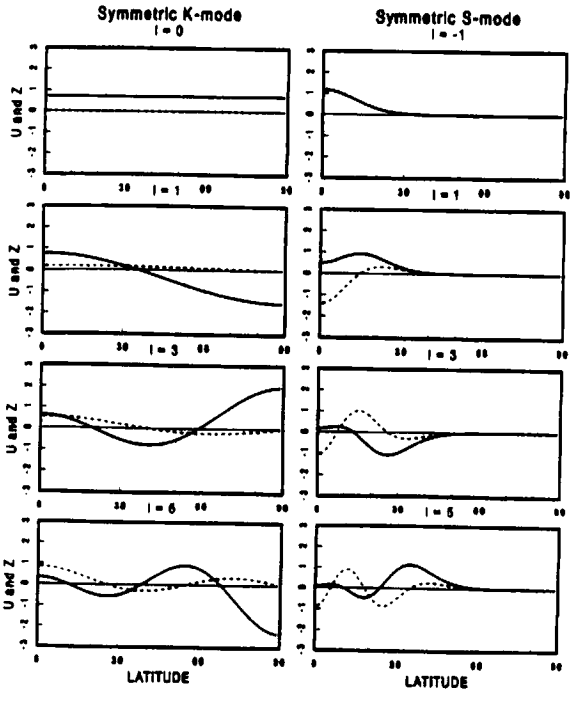

Fig. 1. Meridional structures of symmetric K-modes (left) and S-modes (right) for the internal component at h=150 m. Solid lines denote the dimensionless geopotential Z, and dashed lines the dimensionless zonal wind U. The symbol l denotes a meridional index.

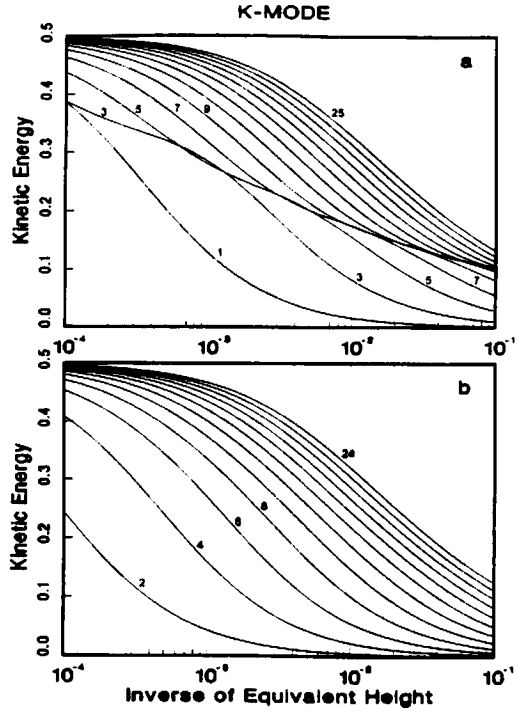

Fig. 2. Normalized kinetic energy of the K-modes as functions of h^{-1}. (a) symmetric modes and (b) antisymmetric modes.

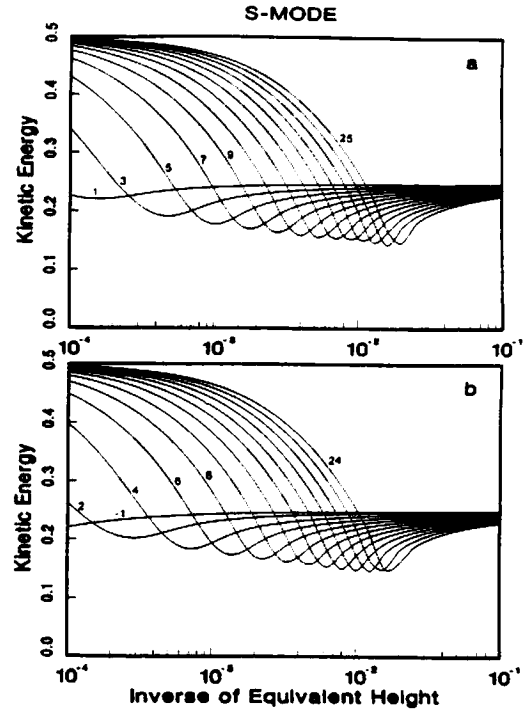

Fig. 3. As in Fig. 2, but for the S-modes. The first symmetric mode l_R= -1 is plotted in (b) with other antisymmetirc modes.

meridional velocity and the dimensionless geopotential, respectively.

The frequencies σ of the rotational modes are identically zero for m=0. This results in V=0, a strictly zonal flow. The required equation to be satisfied by the rotational modes is a geostrophic balance between U and Z. We thus refer to the modes as geostrophic modes.

Kasahara (1978) observed that any combination of U and Z satisfying the geostrophic relation can be a basis function of the geostrophic modes. One such a set of U and Z is constructed by specifying a series of Legendre polynomials, and applied the Gram-Schmidt procedure to obtain an orthonormal set. Hereafter, we refer to these as the K-modes.

Shigehisa (1983) proposed an alternative derivation of geostrophic modes by assuming that $\sigma/m \to c$ as $m \to 0$. The limit c has the analogy of dimensionless phase speed. Given this additional condition at the limit, an eigenvalue problem can be constructed with the eigenvalue c^{-1} from which the normal modes are constructed. Hereafter, we refer to these geostrophic modes as the S-modes.

Figure 1 illustrates the meridional structures of U and Z of symmetric K- and S-modes for h=150 m as an example of internal modes. Note that the differences in their structures between the K- and S-modes are substantial. The structures of the K-modes show large amplitudes of Z compared with those of U and have a global extent with large amplitudes in higher latitudes. In contrast, the structures of S-modes show comparable magnitudes of Z and U and have large amplitudes in low latitudes for low meridional indices. These features resemble those of equatorially trapped internal normal modes of nonzero wavenumbers.

For each Hough vector function so obtained, we define the components of kinetic energy and potential energy by

$$\begin{pmatrix} K_u \\ K_v \\ P \end{pmatrix} = \frac{1}{2} \int_{-\pi/2}^{\pi/2} \begin{pmatrix} U^2 \\ V^2 \\ Z^2 \end{pmatrix} \cos\theta d\theta. \qquad (2)$$

We adopt a normalization condition of $K_u + K_v + P = 0.5$, and K_v=0 for the geostrophic modes.

Figures 2 and 3 describe the normalized kinetic energy levels for the K-modes and S-modes, respectively, as functions of the inverse of equivalent height h. The solid lines for both K- and S-modes indicate a tendency of the energy level approaching 0.5 as h^{-1} decreases. As h^{-1} increases, the kinetic energy level of the K-modes decreases and eventually approaches zero as $h \to 0$. We see for the internal mode at h=10 m that potential energy dominates over kinetic energy, i.e., Z dominates U in their variance. For the S-modes the energy level decreases as h^{-1} increases, as in the case of K-modes. However, we see clear turning points in Fig. 3 such that the K over P ratios approach to unity. It is shown by Shigehisa (1983) that both K and P tend to 0.25 as $h \to 0$. This tendency agrees with that of nonzonal rotational modes. The S-modes share common characteristics with the nonzonal rotational modes, but the K-modes do not have this feature.

3. Atmospheric energy spectrum

In this study, we compare the atmospheric energy spectra by projecting observed data onto these K- and S-modes. Refer to Tanaka (1985) and Tanaka and Kung (1988) for the analysis scheme.

The atmospheric data used are the reanalyzed GFDL FGGE IIIb data for the SOP-1. The twice daily (0000 and 1200 UTC) variables of u, v, and ϕ are given at 12 vertical levels of 1000, 850, 700, 500, 400, 300, 250, 200, 150, 100, 50, 30 mb. The original data at 1.875° latitudinal grids are interpolated onto 60 Gaussian latitudes using cubic spline routines. The vertical structure functions for these 12 vertical levels are constructed numerically according to a finite-difference scheme described by Kasahara and Puri (1981). The vertical mode for k=0 is the external mode, whereas the rest of the vertical modes are the internal modes. Although the higher order vertical

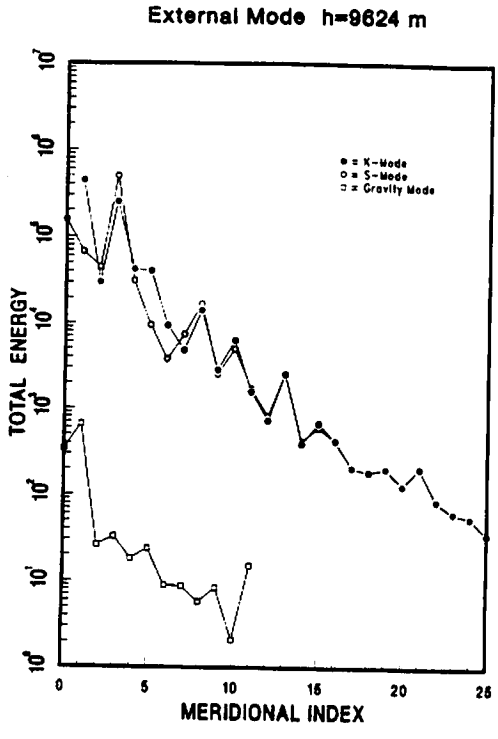

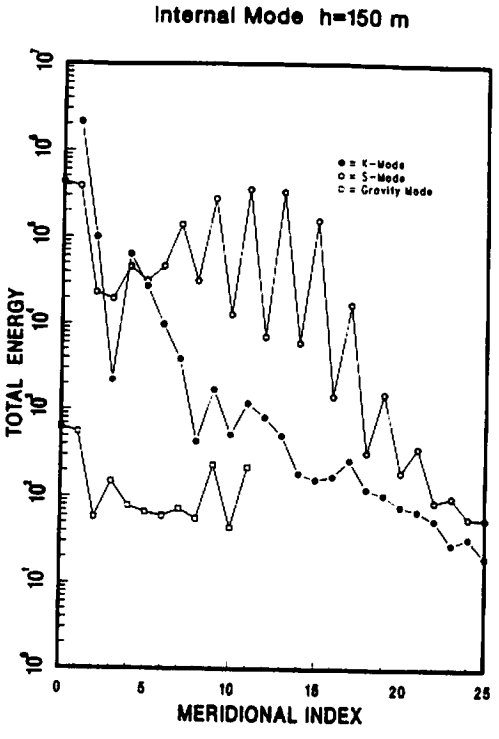

Fig. 4. Spectral distributions of atmospheric total energy of zonal wavenumber zero as functions of the meridional index l. The three panels are for h_k= 9624, 150, and 42 m, respectively. Dots denote for the K-modes, circles for S-modes, and squares for gravity modes. Units are Jm^{-2}.

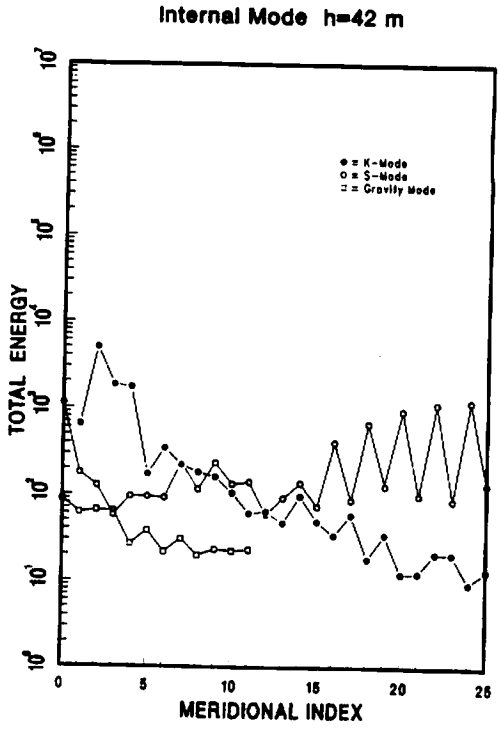

modes are sensitive to the vertical resolution, it should not cause a serious problem for the purpose of comparing K- and S-modes. The energy spectra are evaluated twice daily and averaged for the SOP-1.

The results of the energy spectrum for the zonal wavenumber zero are illustrated in Fig. 4 as functions of the meridional index. The results exhibit the total energy, *i.e.*, the sum of kinetic energy and available potential energy, for K- and S-modes and gravity modes. For convenience, we plotted the projected energy level of l_R=-1 of the S-modes in place of l_R=0. Here the subscript denotes rotational modes. For the external mode (h_k= 9624 m) these two meridional spectra of K- and S-modes are very close to each other, especially in large l_R. The results clearly show that the geostrophic mode energy dominates over the gravity mode energy, confirming that the geostrophic modes are essential for the expansion basis functions. For the internal modes, the energy spectra of K- and S-modes show marked differences with respect to meridional indices. In the case of h_k=150 m, the energy levels of K-modes decrease almost monotonically as l_R increases. The l_R=1 K-mode represents about 90% of the total energy. The energy values of S-modes increase markedly for l_R >7 following an initial decrease in energy levels. This means that several meridional S-modes are necessary to capture the majority of energy, while only the first two K-modes are sufficient. The symmetric S-modes show higher energy levels than the antisymmetric S-modes for l_R >7, and they appear alternately. The alternating appearance of rather large S-modes energy shifts toward a higher meridional index for higher internal modes. The tendency for the data projection onto the S-modes to require many meridional functions becomes more evident for higher internal modes.

The result shows that the symmetric l_R=1 K-mode represents the majority of the total energy of the internal mode. This result may be explained by the fact that structure of Z is suitable for representing the basic meridional geopotential distribution of the atmosphere, having warmer tropics and colder polar regions. In contrast, in order to represent higher latitude structures in terms of the S-modes it is necessary to use many modes of higher meridional indices. The S-modes are suitable to represent evenly partitioned kinetic and potential energies for small

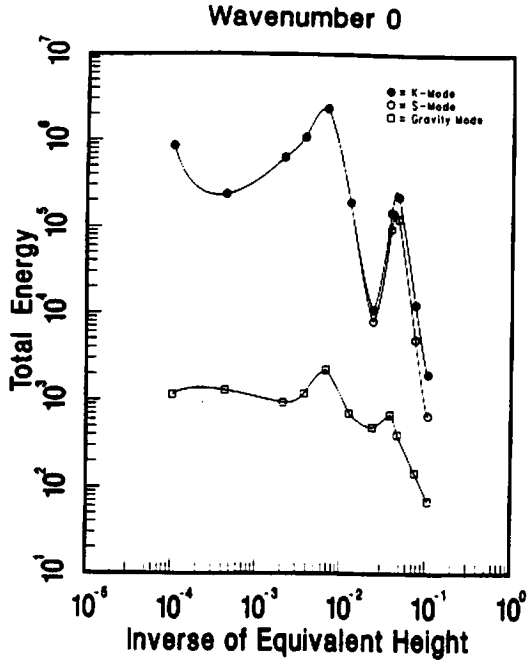

Fig. 5. Vertical energy spectra for n=0 as functions of h_k^{-1}. Dots denote energy projected onto the K-modes, circles denote for S-modes, and squares denote for gravity modes. Units are Jm^{-2}.

h_k. We find that this partitioning is not observed in the atmosphere. The atmospheric zonal fields are fundamentally forced by differential heating. The S-modes, that have the property of free modes, are not effective to describe predominantly forced motions. Therefore, the K-mode series converge faster than the S-mode's to represent observed zonal fields.

Figure 5 illustrates the vertical energy spectra of zonal wavenumber zero as functions of h_k^{-1} for k=0-10. For both the K- and S-mode expansions, the energy maximum (about $23 \times 10^5 Jm^{-2}$) is seen at h_k=150 m. Since the total energy for m=0 is about $60 \times 10^5 Jm^{-2}$, close to one half of the energy is found near the peak at h_k=150 m. The external mode at h_k=9624 m contains $8.4 \times 10^5 Jm^{-2}$. Another energy peak is seen at h_k=22 m. The gravity mode energy is two orders of magnitude less than the geostrophic mode energy. Their energy peaks appear at the same h_k as seen in the geostrophic modes. The energy spectra for K- and S-modes agree well for large h_k. However, the S-mode expansion contains less energy than the K-mode expansion in small h_k due to the slow convergence of the S-modes (see Fig. 4).

4. Concluding remarks

The spectral characteristics of these two different sets of geostrophic modes, which are referred to as K- and S-modes, are compared by projecting atmospheric data onto these modes. The data used in this study is the GFDL reanalyzed FGGE IIIb data.

Both the K- and S-modes indicate similar meridional structures of U and Z components for a large equivalent height such as h_k=9624 m as pointed out by Shigehisa (1983). However, the structures of these geostrophic modes are substantially different for a smaller equivalent height. The K-modes have globally extended structures even for a small equivalent height, whereas the S-modes have equatorially trapped structures. The normalized kinetic energy, K ($=K_n$), and potential energy, P, of these geostrophic modes are compared for a wide range of the equivalent height. We found that $K \rightarrow 0$ and $P \rightarrow 0.5$ as $h \rightarrow 0$ for the K-modes. In contrast, both K and $P \rightarrow 0.25$ as $h \rightarrow 0$ for the S-modes.

A large portion of the atmospheric energy is stored in the zonal energy. The available potential energy dominates over the kinetic energy, and the corresponding wind and mass fields are essentially in geostrophic balance. These observations, resulted from forced motions due to differential heating, match with the characteristics of the K-modes together with the features in the energy ratio and globally extended structures. We found that the K-mode representation captures the majority of observed energy with a few meridional components. The S-modes with the characteristics of free rotational motions and equatorially trapped structures for a small equivalent height are inefficient for the purpose of data expansion. The results show that the use of K-modes is superior to the S-modes in the data representation of zonal atmospheric fields due to a faster series convergence especially for internal modes.

Acknowledgments This research is supported by the National Science Foundation under Grant No. ATM-8923064. Partial support has been provided through the National Oceanic and Atmospheric Administration under No. NA88AANG0140, and the National Aeronautics and Space Administration under Grant No. NAG8-809. NCAR is sponsored by the National Science Foundation.

References

Errico, R. 1989. Theory and Application of Nonlinear Normal Mode Initialization. NCAR Technical Note, NCAR/TN-344+IA. 145 pp.

Kasahara, A. 1977. Numerical integration of the global barotropic primitive equations with Hough harmonic expansions. *J. Atmos. Sci.*, **34**, 687-701.

Kasahara, A. 1978. Further studies on a spectral model of the global barotropic primitive equations with Hough harmonic expansions. *J. Atmos. Sci.*, **35**, 2043-2051.

Kasahara, A. and Puri, K 1981. Spectral representation of three-dimensional global data by expansion in normal mode functions. *Mon. Wea. Rev.*, **109**, 37-51.

Salby, M. L., Garcia, R. R., O'Sullivan, D. and Tribbia, J. 1990. Global transport calculations with an equivalent barotropic system. *J. Atmos. Sci*, **47**, 188-214.

Shigehisa, Y. 1983. Normal modes of the shallow water equations for zonal wavenumber zero. *J. Meteor. Soc. Japan*, **61**, 479-493.

Swarztrauber, P. N. and Kasahara, A. 1985. The vector harmonics analysis of Laplace's tidal equations. *SIAM J. Sci. Stat. Comput.*, **6**, 464-491.

Tanaka, H. 1985. Global energetics analysis by expansion into three-dimensional normal mode functions during the FGGE winter. *J. Meteor. Soc. Japan*, **63**, 180-200.

Tanaka, H. L. and Kung, E. C. 1988. Normal mode energetics of the general circulation during the FGGE year. *J. Atmos. Sci.*, **45**, 3723-3736.

Tanaka, H. L. and Sun, S. 1990. A study of baroclinic energy source for large-scale atmospheric normal modes. *J. Atmos. Sci.*, **47**, 2674-2695.